

Supporting Information

Reverse Transcription Past Products of Guanine Oxidation in RNA Leads to Insertion of A and C opposite 8-Oxo-7,8-dihydroguanine and A and G opposite 5-Guanidinohydantoin and Spiroiminodihydantoin Diastereomers

Anton Alenko, Aaron M. Fleming, and Cynthia J. Burrows*

Department of Chemistry, University of Utah, 315 S 1400 East, Salt Lake City, UT 84112-0850

*To whom correspondence may be addressed.

Phone: (801)585-7290 Email: burrows@chem.utah.edu

Table of Contents

Item	Page
Figure S1. Confirmation of the absolute configurations for the rSp diastereomers in a single-stranded RNA	S2
Figure S2. Example ion-exchange HPLC traces to demonstrate the purity of the Gh-, (S)-Sp, and (R)-Sp-containing RNA strands.	S3
Figure S3. Insertion profiles opposite G and 8-OG in the templates for ProtoScript II, MMLV RT, and AMV RT.	S4
Table S1. Results of nucleotide insertion assays for AMV RT, MMLV RT, and ProtoScript II RT.	S5
Figure S4. Example of data processing for determining initial nucleotide incorporation rates.	S6
Figure S5. Michaelis-Menten plots for insertion of A or G opposite <i>S</i> -Sp, A or G opposite <i>R</i> -Sp, A or G opposite Gh, and C opposite G.	S6
Figure S6. Comparison of extension efficiency by Omniscript RT past OG-A and OG-C base pairs for the OG-1 template.	S7

Table S2. Efficiency of extension past different base pairs formed by OG, Gh, *S*-Sp, and *R*-Sp (analysis of gels from Figure 5). S8

Figure S7. Estimation of nucleotide insertion ratio by PAGE. S9

Figure S8. Estimation of nucleotide insertion ratio by PAGE, gel lane plots. S10

Table S3. Comparison of insertion ratios derived from kinetics and gel-mobility assay. S11

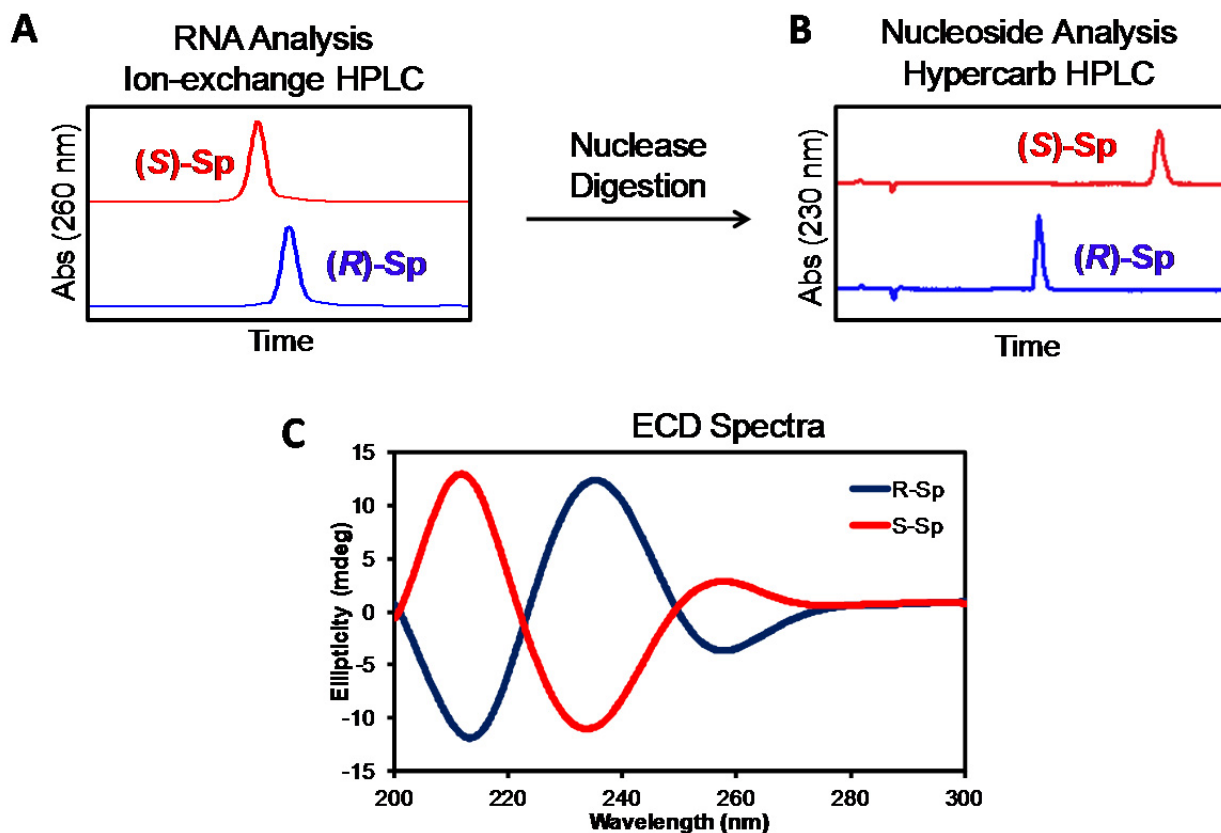


Figure S1. Confirmation of the absolute configurations for the rSp diastereomers in a single-stranded RNA

Previously our laboratory determined the absolute configurations for the Sp diastereomers in short DNA oligomers and 2'-deoxyribonucleosides.¹ Our work noted that the elution order of the dSp diastereomers changed when going from analysis in a short, single strand of DNA analyzed by ion-exchange HPLC vs. dSp in the nucleoside context analyzed by a Hypercarb column. In the present work, we verified the same elution order switching phenomenon occurs in short RNA strands. Confirmation of the absolute configurations for the rSp diastereomers in the RNA templates studied was achieved as follows. First, the RNA strands were purified to contain only one rSp diastereomer using a Dionex DNAPac PA100 (250 x 4.6

mm) ion-exchange HPLC column following a method previously described by our laboratory for dSp in a DNA strand (Figure S1 A).¹ Next, the purified strands were digested to nucleosides using nuclease P1, snake venom phosphodiesterase, and calf intestinal phosphatase following a method previously described by our laboratory.² The nucleosides were then analyzed on a Hypercarb HPLC (150 x 4.6 mm, 5 μ m; Thermo Scientific) column to verify the elution order of the diastereomers switched when compared to the ion-exchange HPLC column (Figure S1 B). Lastly, to confirm the absolute configurations, the individual rSp diastereomeric nucleosides were HPLC purified and then analyzed by electronic circular dichroism (ECD) spectroscopy. The ECD spectra obtained for each rSp diastereomer were identical to those previously obtained for the dSp diastereomers (Figure S1 C).¹ Finally, this confirms that in the RNA templates studied, the first eluting strand has the *S* diastereomer of Sp and the second eluting strand has the *R* diastereomer of Sp.

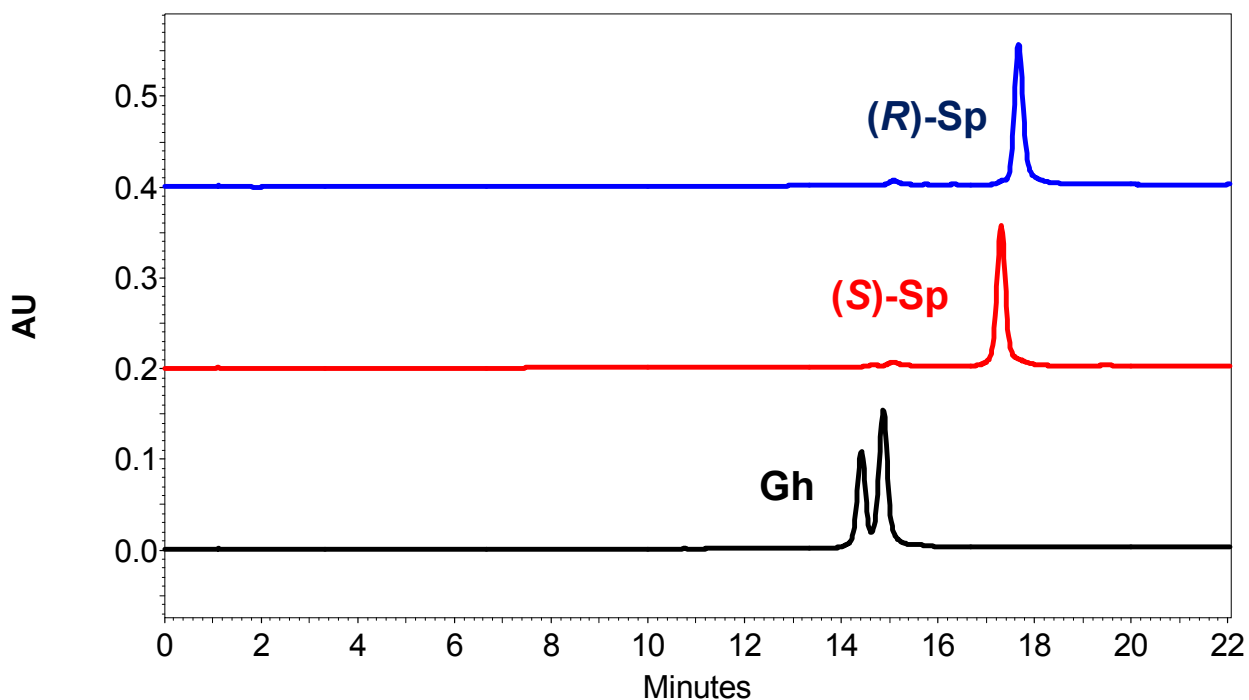


Figure S2. Example ion-exchange HPLC traces to demonstrate the purity of the Gh-, (S)-Sp, and (R)-Sp-containing RNA strands.

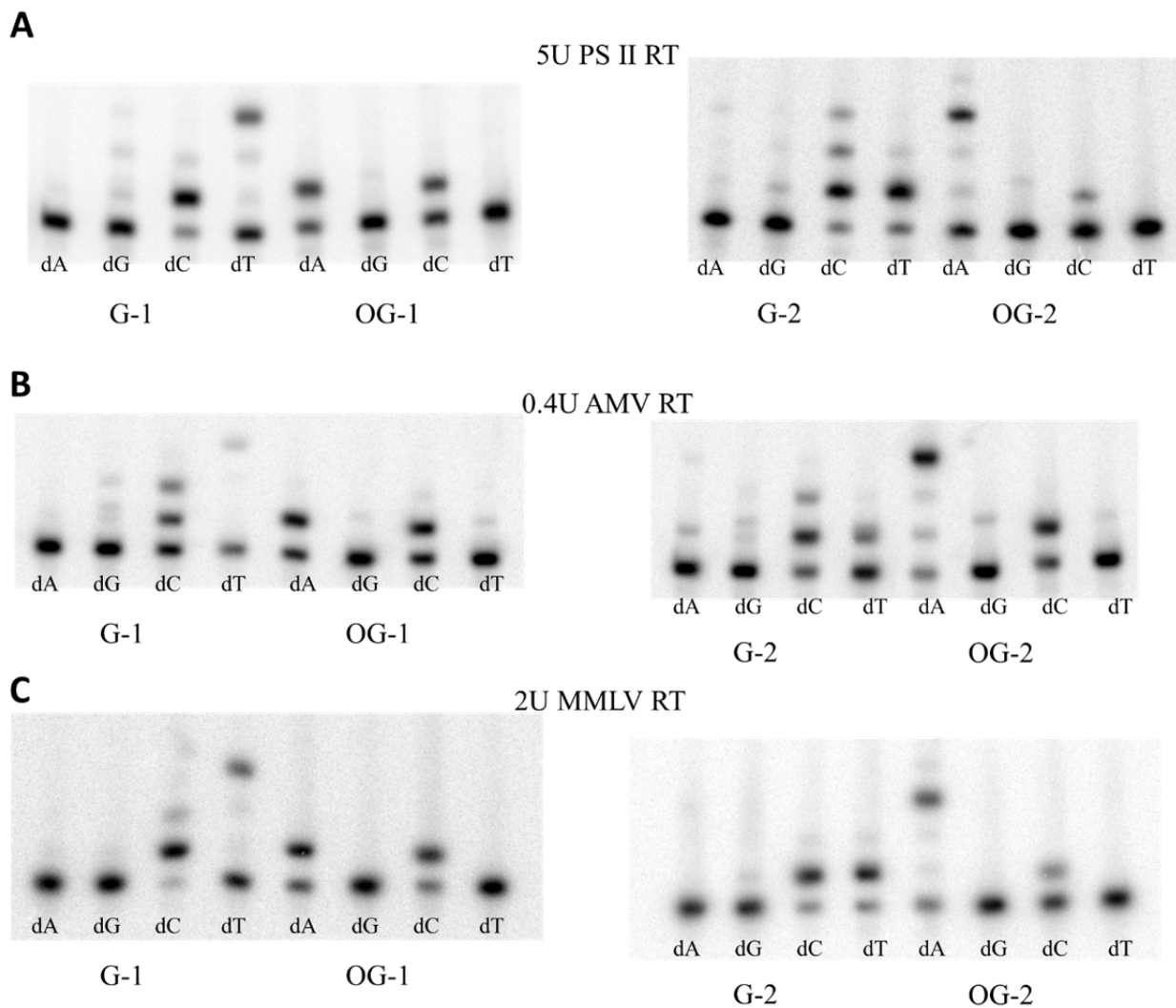
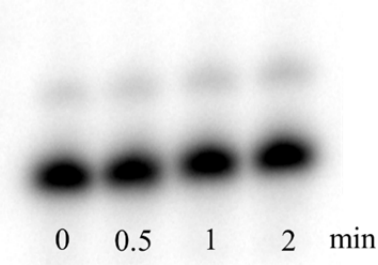


Figure S3. Insertion profiles opposite G and 8-OG in the templates for ProtoScript II (A), AMV RT (B), and MMLV RT (C).

Table S1. Results of nucleotide insertion assays for AMV RT, MMLV RT, and ProtoScript II RT.

		AMV RT				
G-2	C	33%	47%	19%	1%	
	T	60%	37%	2%		
OG-2	A	25%	10%	5%	60%	
	C	42%	58%			
G-1	C	44%	33%	23%		
	T	76%	2%	2%	19%	
OG-2	A	41%	58%	1%		
	C	42%	55%	2%		
		MMLV RT				
G-2	C	21%	75%	4%		
	T	25%	72%	4%		
OG-2	A	37%	4%	3%	53%	3%
	C	70%	30%			
G-1	C	11%	71%	15%	3	
	T	53%	2%	5%	39%	
OG-2	A	36%	64%			
	C	33%	67%			
		ProtoScript II				
G-2	C	18%	50%	20%	12%	
	T	25%	68%	7%		
OG-2	A	50%	9%	4%	35%	2%
	C	78%	22%			
G-1	C	26%	67%	7%		
	T	51%	6%	6%	38%	
OG-1	A	43%	57%			
	C	54%	46%			
		P	P+1	P+2	P+3	P+4

cDNA Separated by PAGE



Reaction Rate Determined from the Gel

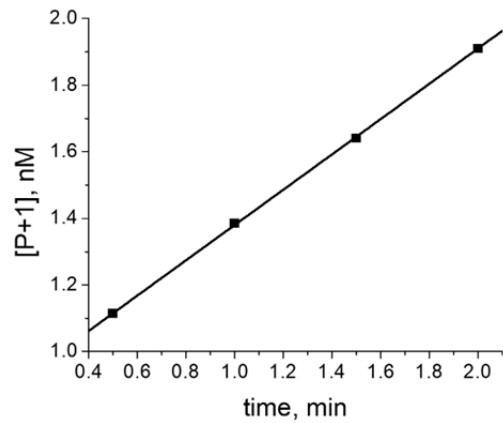


Figure S4. Example of data processing for determining initial nucleotide incorporation rates.

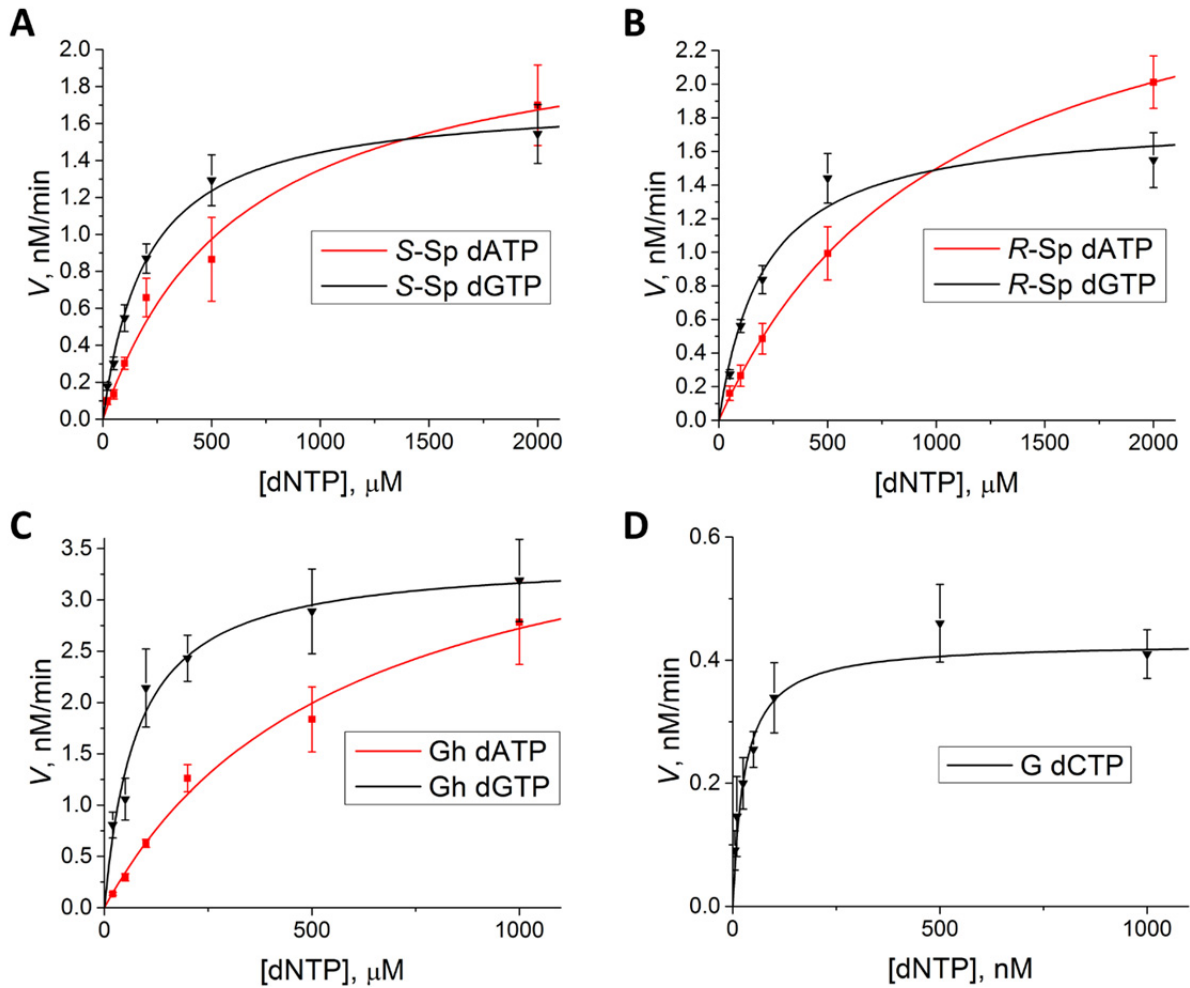


Figure S5. Michaelis-Menten plots for insertion of A or G opposite *S*-Sp (**A**), A or G opposite *R*-Sp (**B**), A or G opposite Gh (**C**), and C opposite G (**D**).

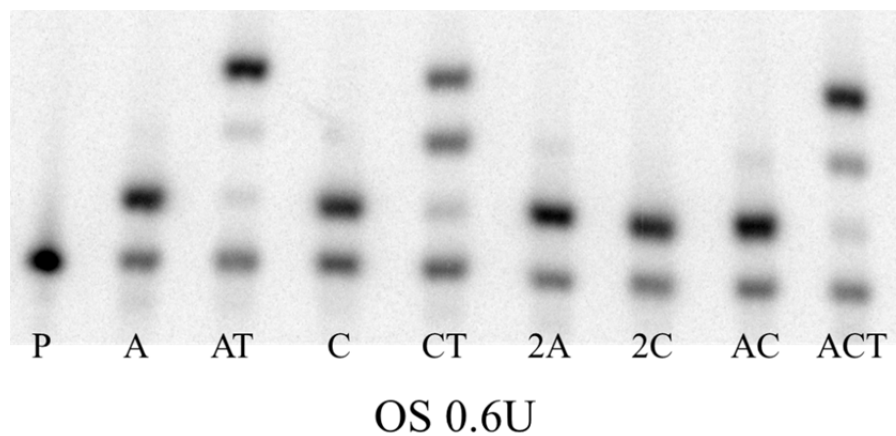


Figure S6. Comparison of extension efficiency by Omniscrypt RT past OG-A and OG-C base pairs for the OG-1 template.

Table S2. Efficiency of extension past different base pairs formed by OG (**A**), Gh (**B**), *S*-Sp (**C**), and *R*-Sp (**D**) (analysis of gels from Figure 5). Tables to the left show fractions of all bands within one lane, tables to the right show fractions of all bands within one lane not accounting for the unextended primer.

A 8-OG

	A	AT	C	CT	2A	2C	AC	ACT
P	27%	27%	33%	27%	23%	28%	26%	23%
P+1	61%	7%	57%	3%	59%	43%	50%	9%
P+2	12%	7%	11%	14%	18%	29%	21%	10%
P+3		52%		53%			3%	52%
P+4		7%		4%				7%

	A	AT	C	CT	2A	2C	AC	ACT
P	-	-	-	-	-	-	-	-
P+1	84%	9%	84%	4%	76%	60%	67%	11%
P+2	16%	10%	16%	19%	24%	40%	29%	12%
P+3		72%		72%			3%	67%
P+4		9%		5%				9%

B Gh

	A	AT	G	GT	2A	2G	AG	AGT
P	28%	31%	26%	22%	23%	21%	21%	19%
P+1	71%	32%	72%	16%	76%	75%	75%	21%
P+2	1%	19%	2%	48%	1%	3%	3%	39%
P+3		16%		14%		1%	1%	19%
P+4		2%		1%				2%

	A	AT	G	GT	2A	2G	AG	AGT
P	-	-	-	-	-	-	-	-
P+1	98%	46%	97%	20%	98%	95%	95%	26%
P+2	2%	28%	3%	61%	2%	4%	3%	48%
P+3		23%		17%		2%	1%	23%
P+4		3%		1%				3%

C *S*-Sp

	A	AT	G	GT	2A	2G	AG	AGT
P	32%	29%	38%	33%	24%	32%	28%	24%
P+1	65%	22%	52%	22%	73%	56%	66%	32%
P+2	3%	16%	6%	21%	3%	8%	4%	14%
P+3		30%	3%	23%		3%	2%	29%
P+4		3%		1%				1%

	A	AT	G	GT	2A	2G	AG	AGT
P	-	-	-	-	-	-	-	-
P+1	96%	32%	84%	33%	96%	83%	91%	42%
P+2	4%	22%	10%	31%	4%	12%	6%	18%
P+3		43%	6%	34%		5%	3%	38%
P+4		4%		1%				2%

D *R*-Sp

	A	AT	G	GT	2A	2G	AG	AGT
P	34%	24%	31%	26%	19%	22%	19%	16%
P+1	64%	26%	64%	29%	78%	72%	77%	30%
P+2	2%	16%	2%	22%	3%	2%	2%	22%
P+3		31%	3%	21%		5%	2%	31%
P+4		4%		2%				3%

	A	AT	G	GT	2A	2G	AG	AGT
P	-	-	-	-	-	-	-	-
P+1	97%	34%	92%	39%	97%	92%	95%	35%
P+2	3%	21%	3%	30%	3%	2%	3%	26%
P+3		40%	5%	28%		6%	3%	36%
P+4		5%		3%				3%

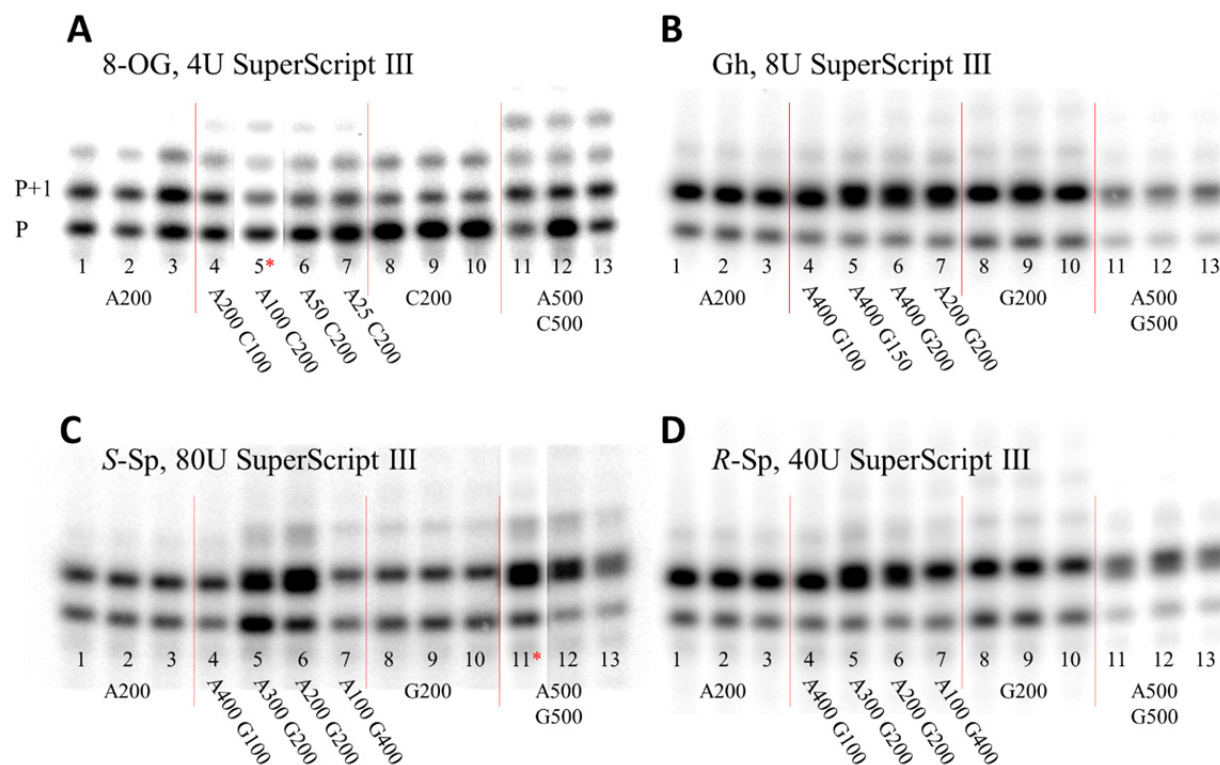


Figure S7. Estimation of nucleotide insertion ratio by PAGE opposite 8-OG (A), Gh (B), S-Sp (C), or R-Sp (D) in the template. Brightness for the lanes marked with * was adjusted separately from the rest of the gel.

Primer extension was performed as described in materials and methods using indicated amount of SuperScript III reverse transcriptase in 20 μL. On the gels lanes 1-3 correspond to reactions containing 200 μM dATP, lanes 8-10 – 200 μM dCTP or dGTP, lanes 11-13 – 500 μM mixture of dATP and dCTP or dGTP, lanes 4-7 – different ratios of dATP and dCTP or dGTP (indicated on the gel in μM).

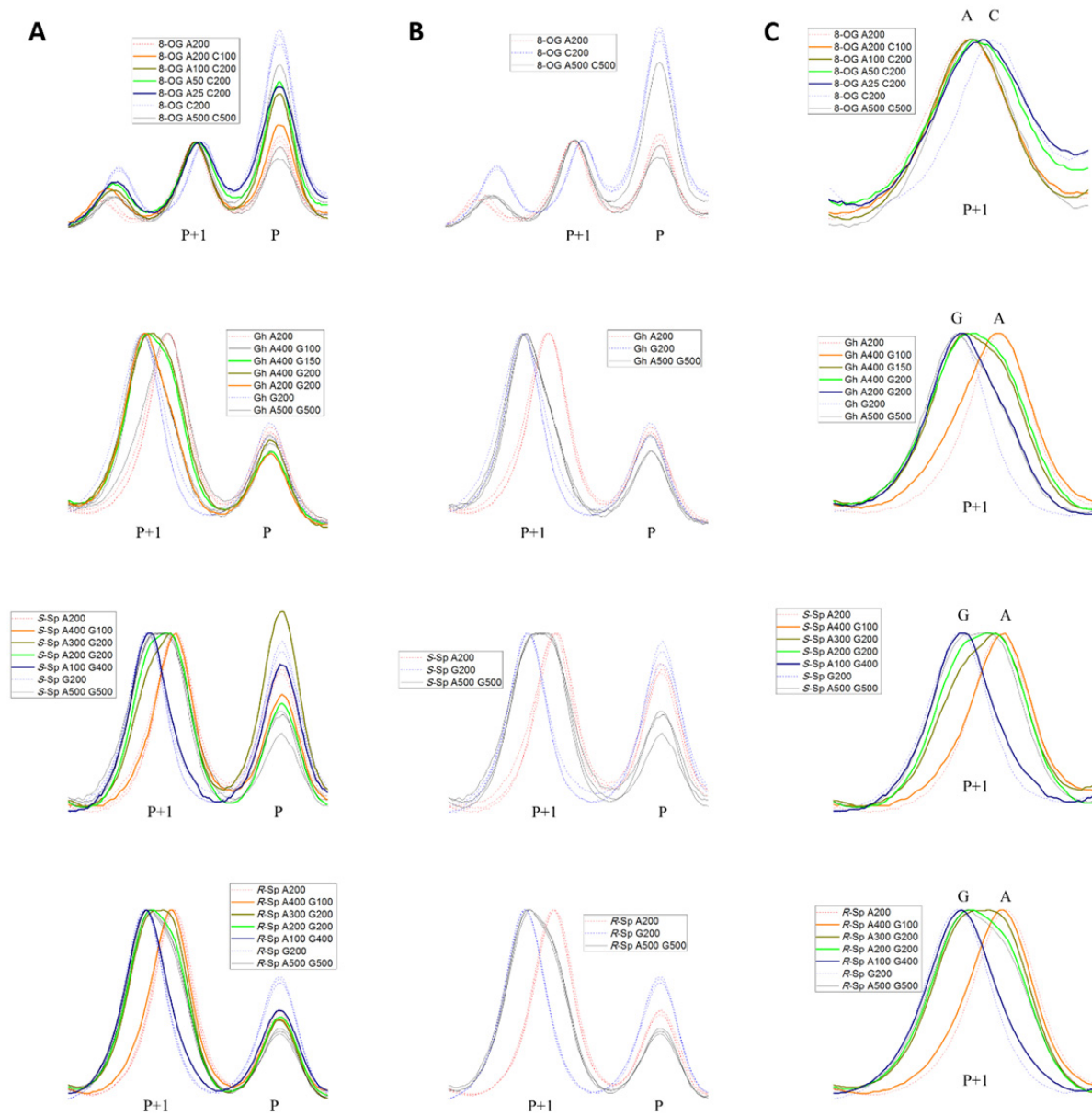


Figure S8. Estimation of nucleotide insertion ratio by PAGE, gel lane plots. **A** – combined plots of all lanes showing alignment; **B** – plots of lanes done in triplicate (1-3, 8-10, and 11-13) showing reproducibility of relative peak positions; **C** – plots of P+1 peak showing ratios of insertion of A and C or G at different dNTPs concentrations (only one representative peak is shown for the samples done in triplicate).

Table S3. Comparison of insertion ratios derived from kinetics and gel-mobility assay. “Calculated insertion ratio” – insertion ratio calculated from steady-state kinetic parameters for the given concentrations of dNTPs. “RSD” – relative standard deviation, “SD” – standard deviation, “# of SD to 1:1” – how many standard deviation intervals it would take to make calculated insertion ratio 1:1.

		[dNTP], μM	Actual insertion ratio	Calculated insertion ratio	RSD*	SD	# of SD to 1:1
OG	dCTP	200	1	2.5	19%	0.48	4
	dATP	25	1	1			
Gh	dGTP	200	1	1.4	32%	0.46	1
	dATP	400	1	1			
S-Sp	dGTP	200	1	1.6	26%	0.42	2
	dATP	200	1	1			
R-Sp	dGTP	200	1	1.3	27%	0.5	1
	dATP	300	1	1			

*-calculated based on propagation of error for $k_{\text{cat}} * K_M' / (k_{\text{cat}} * K_M)$

References

- (1) Fleming, A. M., Orendt, A. M., He, Y., Zhu, J., Dukor, R. K., and Burrows, C. J. (2013) Reconciliation of chemical, enzymatic, spectroscopic and computational data to assign the absolute configuration of the DNA base lesion spiroiminodihydantoin, *J. Am. Chem. Soc.* **135**, 18191-18204.
- (2) Chen, X., Fleming, A. M., Muller, J. G., and Burrows, C. J. (2013) Endonuclease and exonuclease activities on oligodeoxynucleotides containing spiroiminodihydantoin depend on the sequence context and the lesion stereochemistry, *New J. Chem.* **37**, 3440-3449.